ACS APPLIED MATERIALS & INTERFACES

Research Article

Cite This: ACS Appl. Mater. Interfaces 2018, 10, 43343−43351

www.acsami.org

Electrochemical Determination of Adrenaline Using MXene/Graphite Composite Paste Electrodes

S. Sharath Shankar,*[,†,‡] Rayammarakkar M. Shereema,[†] and R. B. Rakhi*[,†]

[†]Chemical Sciences and Technology Division, CSIR-National Institute of Interdisciplinary Science and Technology (CSIR-NIIST), Thiruvananthapuram, Kerala 695019, India

[‡]Department of Biochemistry and Molecular Biology, School of Biological Sciences, Central University of Kerala, Kasargod 671314, India

Supporting Information

ABSTRACT: MXene/graphite composite paste electrode (MXene/GCPE)-based electrochemical sensor has been fabricated for the detection of adrenaline. The electrode exhibits a sensitive response to adrenaline in phosphate buffer solution of pH 7.4, and its catalytic activity is much higher than that of the bare graphite paste electrode. The electron-transfer reaction of MXene/GCPE is a diffusion controlled process. The graph of concentration of adrenaline with the peak current exhibits two linearities, one in the lower and other in the higher concentration range with a detection limit of 9.5 nM. The simultaneous analyses of adrenaline, ascorbic acid, and serotonin reveal that the fabricated electrode could separate the overlapped cyclic voltammetric peaks of these ternary mixtures. This electrode has been further employed in the detection of adrenaline in pharmaceutical samples with 99.2−100.8% recoveries.

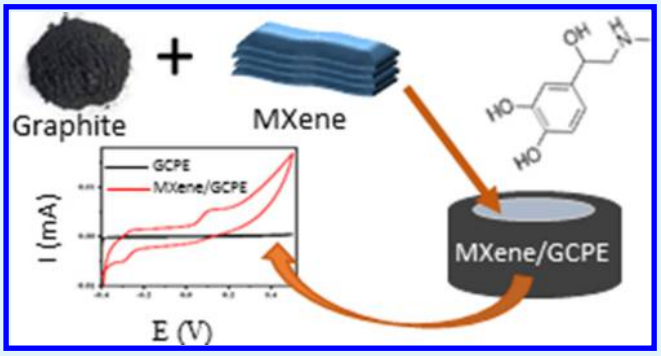

KEYWORDS: *MXenes, MXene/graphite composite, cyclic voltammetry, adrenaline, detection limit*

INTRODUCTION

Recently, MXenes, a new family of two-dimensional (2D) materials prepared by the chemical exfoliation of MAX phases (transition metal carbides and carbonitrides) are attracting significant research attention because of their unique structural and electronic properties.[1−3] Immersing of hexagonal titanium aluminium carbide MAX phase ($T_{n+1}AlC_n$) in HF solution results in the selective removal of the Al layer and leads to the formation of the layered titanium carbide, surface terminated with weakly bonded −OH or −F groups ($Ti_{n+1}C_nT_x$, where T_x stands for a general surface termination).[4−6] The widely explored MXene in this group to date, $Ti_3C_2T_x$, has demonstrated its potential as an excellent electrochemical transducer for electrochemical sensing applications.[7−9] Wang et al. reported the use of organ-like $Ti_3C_2T_x$ MXene nanolayers as a hemoglobin immobilization matrix.[8] Rakhi et al. reported a highly sensitive amperometric glucose biosensor with Au nanoparticles dispersed $Ti_3C_2T_x$ MXene as the enzyme immobilization matrix.[10] In all these studies,[7−10] the MXene nanosheets provided a suitable environment for the respective proteins to retain their stability and activity. So far, no reports are available on the electrochemical sensing properties of the lightest MXene, Ti_2CT_x.

Adrenaline (AD) a catecholamine is a sympathetic neural and hormonal transmitter substance present in most mammalian species.[11,12] They are released from the adrenal medulla and perform many functions like a regulator of blood pressure, vasoconstriction, heart rate, and bronchodilator for asthma.[13,14] Usually, the AD is released during emotional or physical stress, which causes the sympathoadrenal system to increase the concentration of AD in blood. Adrenaline in early stages has been used for cardiopulmonary resuscitation, defibrillation, and also in cardiac arrest for decades.[14−16] Hence, the quantification of adrenaline in biological samples is attracting substantial research interest recently.[17−19]

Being catecholamine, AD is electrochemically active and can detect them using electro analytical techniques.[20,21] The major problem associated with the electrochemical determination is the closeness of the oxidation potential of AD with the other biological molecules such as ascorbic acid (AA), serotonin (5-hydroxytryptamine or 5-HT), and so forth.[22,23] Hence, its detection in real samples is very difficult, and most of the time, the results are obtained with ambiguity. Moreover, in a biological fluid like blood, the concentration of AD lies in the micromolar range and the lifetime of these neurotransmitters in the extra cellular space is short because of metabolism and cellular uptake.[24,25] Hence, it is rattling essential to produce an electrochemical sensor which can detect the minute concen-

Received: July 17, 2018
Accepted: November 22, 2018
Published: November 22, 2018

DOI: 10.1021/acsami.8b11741
ACS Appl. Mater. Interfaces 2018, 10, 43343−43351

trations of AD in various samples such as blood, urine, and so forth. Most of the AD sensors are based on carbon nanotubes (CNTs), graphene, graphite, or nanocarbon electrodes.[23,25] In the present work, for the first time, we report the fabrication and electrochemical performance studies of a highly sensitive AD sensor based on a novel MXene/graphite composite paste electrode (GCPE).

EXPERIMENTAL SECTION

Reagents. Analytical grade chemicals were used for the work without any further purification. 100 mM perchloric acid was used for the preparation of AD hydrochloride and serotonin hydrochloride stock solutions. Double distilled water was used for the preparation of the AA stock solution. Phosphate buffer solution (PBS) of different pH was prepared by mixing sodium dihydrogen phosphate and disodium hydrogen phosphate as per the standard procedure. AD hydrochloride, AA, and serotonin hydrochloride were purchased from Sigma-Aldrich, Milwaukee, WI, USA. All the chemical solutions were prepared in double distilled water, and the experiments were performed at room temperature.

Synthesis of Ti_2CT_xMXene. 2D Ti_2CT_xMxenes were prepared by the selective removal of Al layer from the commercially available Ti_2AlC (Maxthal 211) powder by the procedure reported in our earlier work.[26] The Maxthal powder was immersed in 10% HF for 10 h at room temperature. The resulting suspension was washed with deionized water several times and then filtered to get 2D Ti_2CT_xMXenes. The as-prepared MXenes were then annealed in the N_2 atmosphere for 2 h at 500 K.

Preparation of MXene/GCPE. MXene/GCPE was prepared by grinding different ratios of MXene with 70% of graphite powder and 30% of silicon oil in an agate mortar for 30 min. Thus obtained homogeneous mixture was further packed into the cavity of a homemade electrode, and the electrode surface was smoothened with a weighing paper. Similarly, a bare GCPE was prepared by the same procedure without adding MXene.

Optimization of the Amount of MXene in the Electrode. To optimize the amount of MXene required for the preparation of MXene/GCPE with maximum sensitivity, MXene with weight ranging from 5 to 30 mg were added to the mixture of 0.24 g of graphite powder and 0.3 mL of silicone oil. The electrochemical performance of fabricated electrode prepared from each combination was studied by using ferri/ferrocyanide redox probe.[27] It was observed that the electrochemical cathodic (I_{pc}) and anodic peak current (I_{pa}) were enhanced up to 15 mg. The current against the amount of MXene was plotted (Figure S1), and from the plot, it was observed that the oxidation peak of the redox probe on modifier electrode was enhanced upto 15 mg of the MXene, anything beyond that quantity tends to decrease the sensitivity. Hence, the composite paste electrode with 15 mg of MXene was used for further analysis.

Characterization. The crystal structure samples were characterized from X-ray diffraction (XRD) patterns recorded on a Philips X'pert diffractometer (XRD, X'Pert Pro MPD) with Cu Kα radiation (λ = 1.5406 Å). The morphological analysis of the samples was carried out using a scanning electron microscope (SEM), (JEOL, model JSM 5600 LV, Tokyo, Japan). A high-resolution transmission electron microscope (FEI, Tecnai S TWIN microscope) with an accelerating voltage of 300 kV was used for the microstructural evaluation. The electrochemical measurements were conducted in a three-electrode configuration consisting of a working electrode (MXene/GCPE, 3 mm in diameter), Pt wire counter electrode, and saturated calomel electrode as the reference electrode, using an electrochemical workstation (VMP3-Bio-Logic electrochemical workstation).

RESULTS AND DISCUSSIONS

Figure 1a,b, respectively, shows the XRD patterns of the as-received Maxthal 211 powder (Ti_2AlC) and the N_2 annealed Ti_2CT_xMXene (Ti_2CT_x-N_2). The major peaks in the XRD

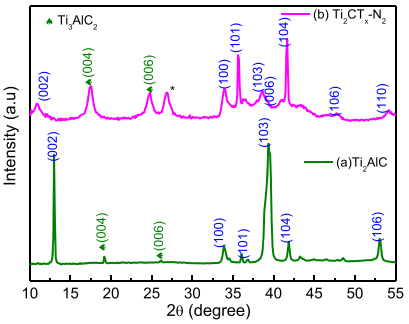

Figure 1. XRD patterns of (a) as-received Maxthal 211 powder (Ti_2AlC) and (b) N_2 annealed Ti_2CT_xMXenes (Ti_2CT_x-N_2).

pattern of Maxthal sample can be readily indexed to the hexagonal Ti_2AlC MAX phase (JCPDS card no. 00-029-0095). The pattern also contains two minor peaks corresponding to Ti_3AlC (JCPDS card no. 52-0875) which is present in the sample as a secondary phase. The peaks get shifted to lower 2θ values, indicating the increase in interlayer spacing of MXenes after the removal of Al layer by HF-treatment. The broadening of peaks indicates the decrease in crystallinity and multilayer nature of MXenes.[2,3,26,28] The local heat generation during the etching process leads to the presence of a small amount of anatase TiO_2 (JCPDS card no. 00-021-1272) in the Ti_2CT_xMXene sample.

A detailed comprehensive study on the structural and electrochemical properties of Ti_2CT_xMXene annealed at different ambient conditions proved that annealing of HF-treated Ti_2AlC MAX phase at different ambients helps in further tuning of the MXene structure to improve its physical properties.[26] While annealing in air oxidizes the MXene samples and convert them into a composite of graphitic carbon nanoflakes and TiO_2 nanocrystals, annealing in Ar or N_2 atmosphere helps in retaining the original structure and morphology of MXene. As compared to the sample annealed in Ar, MXene annealed in N_2 has the lower concentration of fluoride ions, which helps in the improvement of the electrochemical properties of MXene samples.

Ease of preparation, wide potential range, low background current, ability to introduce various modifiers during paste preparation, easy removal of electrode surface layer, low Ohmic resistance, no need for pretreatment and low cost were the primary criteria for the election of the graphite powder for the preparation of MXene/GCPEs. Moreover, graphite powders have high porosity and can prepare a homogenous mixture with the MXene by the manual grinding procedure. During this process, the surface areas of both the graphite and MXene particles will get enhanced. The electrocatalytic properties of electrode prepared by this composite will be higher due to the enhancement in the electroactive surface area.

Morphology and microstructure of the graphite, MXene, and MXene/graphite composite were analyzed using SEM. Figure 2 shows the SEM images of (a) graphite powder, (b) MXene, and (c) MXene/graphite composite paste. The graphite powder contains micrometer-sized flakes with irregular shapes. SEM image of the N_2-annealed HF-treated MAX phase (Ti_2CT_x-N_2MXene sample) (Figure 2b) reveals that the Al layer is removed from the Ti_2AlC MAX phase upon the etching process, leading to the formation of stacked MXene sheets resembling the structure of exfoliated graphite.[29] The

DOI: 10.1021/acsami.8b11741
ACS Appl. Mater. Interfaces 2018, 10, 43343−43351

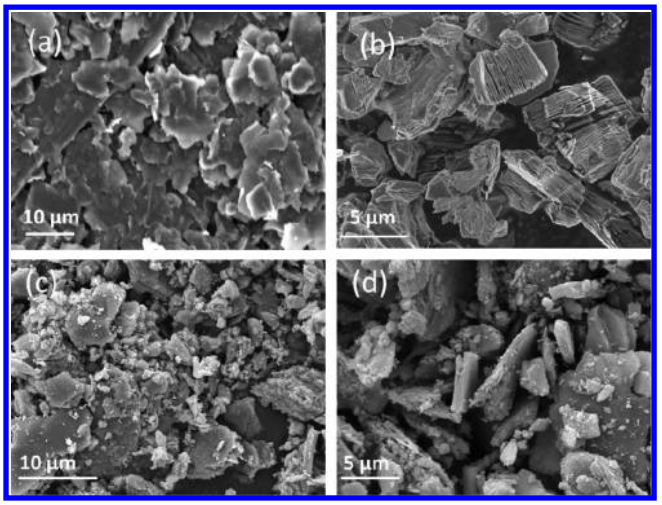

Figure 2. SEM image of (a) graphite powder, (b) N_2 annealed HF-treated MAX phase (Ti_2CT_x-N_2 MXene sample), and (c,d) MXene/graphite composite paste.

average size of MXene flake is nearly 5 μm. The presence of both graphite and MXene are identified from the SEM images of the composite shown in Figure 2c,d. The two components are well mixed in the composite paste.

The microstructure of the MXene sheet is analyzed using transmission electron microscopy (TEM) (Figure 3a). TEM

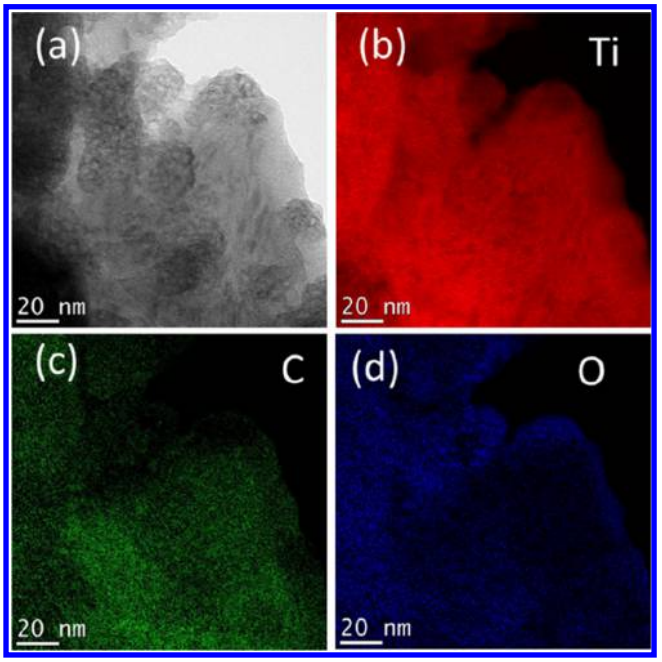

Figure 3. (a) TEM image of MXene sample annealed in N_2 atmosphere (Ti_2CT_x-N_2 MXene) and elemental mapping of (b) Ti, (c) C, and (d) O in the MXene sheets.

image shows thin and transparent MXene sheets having many nanometer-sized holes on the surface. A similar feature has been reported for functionalized graphene.[21] The spatial distributions of the elements Ti, C, and O on the N_2 annealed MXene samples are studied using energy-dispersive spectrometer elemental mapping, and the results are shown in Figure 3b–d respectively. The oxygen comes from the functional groups attached to the surface of MXene sheets.

High-resolution TEM image of MXene/graphite composite is shown in Figure 4a. TEM image indicates that the sample

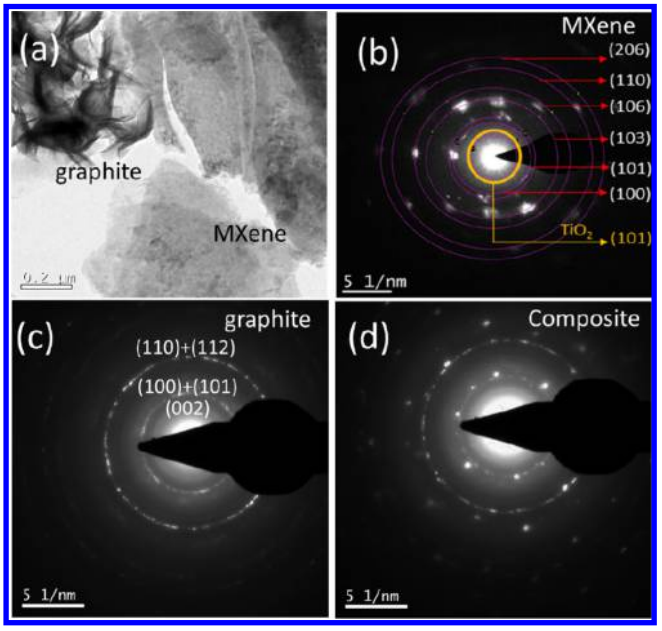

Figure 4. (a) TEM image of the MXene/graphite composite and selected area electron diffraction patterns of (b) MXene nanosheets, (c) graphite nanoflakes and (d) MXene/graphite composite.

contains thin and transparent layers of both MXene sheets and graphite flakes, which can be easily differentiated from each other. The vigorous sonication of the composite during the TEM sample procedure separates the stacked layers of MXenes as well as graphite. The selected area diffraction (SAED) pattern corresponding to area containing MXene sheets alone in the composite is shown in Figure 4b. The SAED pattern confirms that the MXene sheets preserve the crystallinity and hexagonal symmetry of the as-received Ti_2AlC MAX phase. The SAED pattern is indexed to the hexagonal Ti_2AlC MAX phase crystal structure using circular Hough diffraction analysis.[30] The pattern also contains one reflection peak from body-centered tetragonal anatase TiO_2, produced by the local heat evolved during the preparation of the MXene. TEM results agree well with the results obtained from the powder XRD analyses. Figure 4c shows the SAED pattern corresponding to the area containing graphite flakes only. The pattern indicates that the flake structure is crystalline and it matches that of crystalline graphite. The diffraction from (002) plane is very weak, indicating the paucity of stacked graphite sheets.[31] Figure 4d shows the SAED pattern of the MXene/graphite composite corresponding Figure 4a. The pattern contains the diffraction rings from both the components (MXene and graphite).

Cyclic voltammetric (CV) experiments were performed for studying the catalytic capability of MXene/GCPE by using $K_3Fe(CN)_6$ in the KCl electrolyte system. The cyclic voltammograms recorded with bare GCPE, and MXene/GCPE in 1 mM $K_3[Fe(CN)_6]$ with 0.1 M KCl supporting electrolyte was depicted in Figure 5. On the bare GCPE, the anodic and cathodic peaks were observed at 223 and 165 mV, respectively. At the MXene/GCPE, a drastic enhancement in the peak current was observed with a small shift in peak potentials (E_{pa} = 251, E_{pc} = 187 mV). The potential difference

DOI: 10.1021/acsami.8b11741
ACS Appl. Mater. Interfaces 2018, 10, 43343–43351

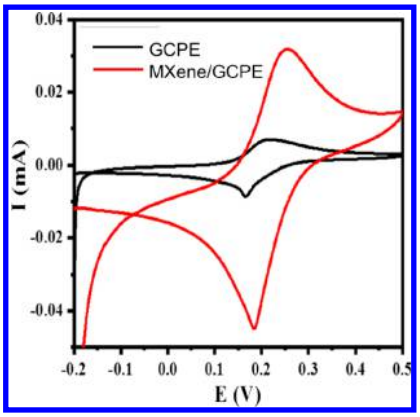

Figure 5. CVs of GCPE, MXene/GCPE in 1 mM $K_3Fe(CN)_6$ and 0.1 M KCl with a scan rate 50 mV s^{-1}.

of (ΔE_p) 58 mV at the bare GCPE and 64 mV at the MXene/GCPE indicates that a reversible redox reaction is taking place at both the electrodes. The effective surface areas of bare and modified electrodes were calculated through the plot of CVs of redox probe with different scan rates (Figures S2a,b and S3a,b), and it is found to be 0.0015 cm^2 for the bare and 0.0129 cm^2 for the modified electrode. The increase in peak currents on the modified electrode could be justified from the enhanced electrochemical surface area of the fabricated electrode.[32]

The changes in the impedance upon electrode surface modification process is studied using electrochemical impedance spectroscopy (EIS) measurements conducted in 0.1 M $[Fe(CN_6)^{3-/4-}]$ electrolyte. Figure S4 shows the EIS spectra or the Nyquist plots obtained for GCPE and MXene/GCPE electrodes. For both the electrodes, the individual Nyquist plot consists of two distinct regions. The semicircular arc at the high-frequency region represents the electron-transfer limited process, and the linear part at low-frequency region corresponds to the diffusion-limiting step of the electrochemical process.[33,34] The *X*-intercept of the Nyquist plot gives the solution resistance (R_s). R_s for GCPE and MXene/GCPE are measured as 2.3 and 1.3 Ω, respectively. The diameter of semicircle gives the value of the electron charge transfer resistance R_{ct}. The R_{ct} values for GCPE and MXene/GCPE are 1000 and 300 Ω, respectively. The lower R_{ct} value of the MXene/GCPE composite electrode indicates that the incorporation of the MXene nanosheets increases the electronic conductivity of the composite electrode and improves the electron-transfer process. The diffusion-controlled process (Warburg diffusion) occurring at the electrode/electrolyte interface, in the low-frequency region is a mass transfer process, in which electrolyte ions diffuse into the electrode.[35] The lower inclination of the line from the vertical in the low-frequency region for the MXene/GCPE as compared to bare GCPE indicates that the composite electrode surface offers lower resistance (Warburg impedance, *W*) of the ion permeability. The Randles equivalent circuit of the sensor electrode is shown as the inset of Figure S4. In addition to the resistances, the circuit consists of a double-layer capacitance C_{DL}, corresponding to the dielectric characteristics at the electrode/electrolyte interface.

The capability of the MXene/GCPE toward the electrochemical determination of AD was checked by using CV. The effect of scan rates on the electrocatalytic properties of the bare and modified electrodes toward the AD oxidation was investigated. Figures 6a and S5a show the CV curves of oxidation of AD with different scan rates (50−140 mV s^{-1}) at

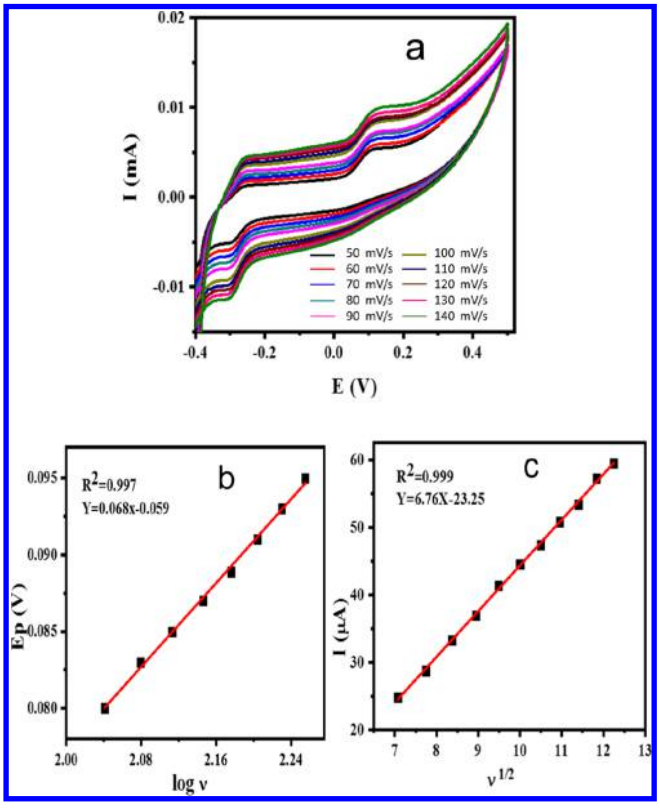

Figure 6. (a) CVs of 1.0 μM AD in 0.2 M PBS of pH 7.4 at MXene/GCPE with various scan rates (from 50 to 140 mV s^{-1}) (b) plots of E_{pa} vs log of scan rates (c) plots of I_{pa} vs square roots of scan rates.

the MXene/GCPE and bare GCPE, respectively. It was also observed that while increasing the scan rate, the AD oxidation peak current was getting increased with a shift in potential toward the positive side was experienced. This behavior suggests the kinetic limitation of the reaction between the active sites of AD and that of the modified electrode. Moreover, the increased current rate was observed with the increase in scan rate because during the higher scan rate, the electrode surface will get sufficient time for executing their catalytic activity toward the analyte.[36] The peak potential versus log scan rate was also plotted (Figures 6b and S5b), and the slope was calculated as 0.51 and 0.48, respectively. From this graph, the electron-transfer coefficient (α) for both modified and bare electrodes was calculated as 0.43 and 0.06, respectively.[32] The plot of the square root of scan rates with peak current (Figures 6c and S5c) shows a linear relationship with a correlation coefficient of 0.999 at MXene/GCPE and 0.998 at GCPE. Using this graph, the diffusion coefficient of the MXene/GCPE was calculated as 0.379 cm^2 s^{-1}, whereas it is calculated as 0.119 cm^2 s^{-1} for the bare GCPE.[36,37] The results indicate that the electrochemical reaction was controlled by diffusion process on the fabricated electrode.[38]

Figure 7a shows the comparison of CVs of the bare and the modified electrodes in 0.1 μM AD in 0.2 M PBS of pH 7.4. Both the electrodes were scanned from a potential of −0.4 to 0.5 V at a scan rate of 50 mV s^{-1}. The poor sensitivity exhibited by the bare GCPE toward redox reaction of AD was

DOI: 10.1021/acsami.8b11741
ACS Appl. Mater. Interfaces 2018, 10, 43343−43351

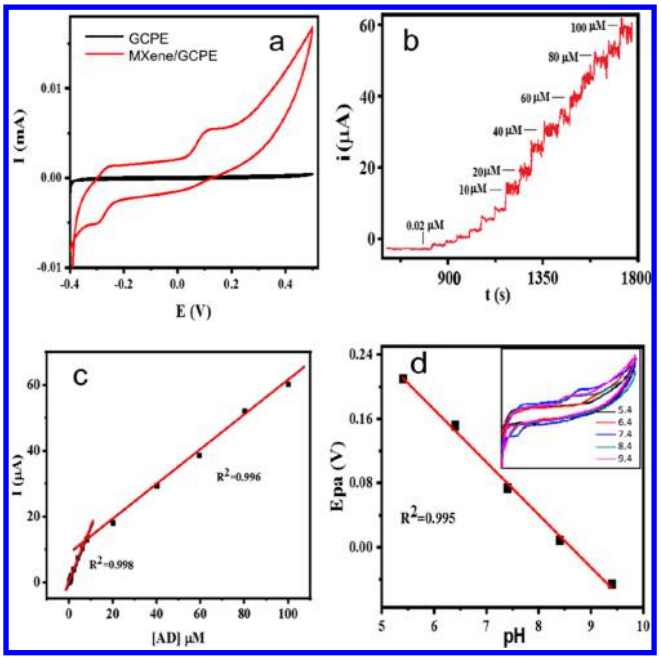

Figure 7. (a) CVs of 1.0 μM AD in 0.2 M PBS of pH 7.4 at GCPE (curve a) and at MXene/GCPE with a scan rate of 50 mV s^{-1}. (b) Chronoamperometric responses for the increasing concentrations of AD with a time interval of 30 s in 0.1 M PBS at 1.2 V. (c) Plot of concentration of AD vs current. (d) Graph of anodic peak potential vs pH. (Inset) CVs obtained for 1.0 μM AD with the MXene/GCPE in 0.2 M PBS with pH values, (a) 5.4 (b) 6.4 (c) 7.4 (d) 8.4, (e) 9.4, at scan rate of 50 mV s^{-1}.

improved considerably upon modification. On the developed electrode, both the oxidation and reduction peak currents of AD enhanced up to 100 folds. The enhancement in the electrocatalytic current is attributed to the high conductivity offered by the MXene. The enhanced catalytic activity may be due to the porous interfacial layers of the MXene present on the modified electrode, which increases the conductive area of the electrode because of its high specific surface area. Higher sensitivity and selectivity of the fabricated electrode were attributed to the fact that the AD molecule could interact through the conductive porous channels onto the electrode more easily.[39] As a result of this interaction, positively charged AD (7.4 pH) undergoes oxidation at a relatively low potential and form adrenoquinone. The corresponding current was measured with an accuracy of $\pm$0.01 μA. The concentration studies with a modified electrode revealed that both the oxidation and reduction peak currents were increased with the increase in the concentration of AD. Chronoamperogram of the AD with various concentrations in PBS (pH 7.4) with a 30 s time interval at a potential of 1.2 V is shown in Figure 7b. The current obtained from chronoamperometry was plotted against the concentration of AD (Figure 7c), and the resultant plot exhibits two linearities, one in the lower concentration range (0.02−10 μm) and other in the higher concentration range (10−100 μm).[40] From this plot, the lower detection limit of the modified electrode toward AD is calculated as 9.5 nM. The effect of pH on the voltammetric determination of AD with modified electrode was examined over various pH range ranging from 5.4 to 9.4. From Figure 7d (inset), it is found that the oxidation peak current and peak nature largely depend on the pH of the solution. The plot of E_p versus pH (Figure 7d) reveals that, as pH of solutions changes from lower to higher pH values, a shift in peak potentials toward the negative side was experienced. The slope of the plot is calculated as −57 mV/pH, suggesting the participation of the same number of electrons and protons in the redox reactions of AD.[41] It is also observed that the peak current increases with increasing pH from 5.4 to 7.4 and a maximum current response is obtained for 7.4 pH, and further increase in pH aids to decrease the peak current. Therefore, PBS with 7.4 pH is chosen as the optimum pH for further evaluation.

Figure 8a shows the electrochemical behavior of 5-HT at bare and modified electrodes in PBS. On bare GCPE, the

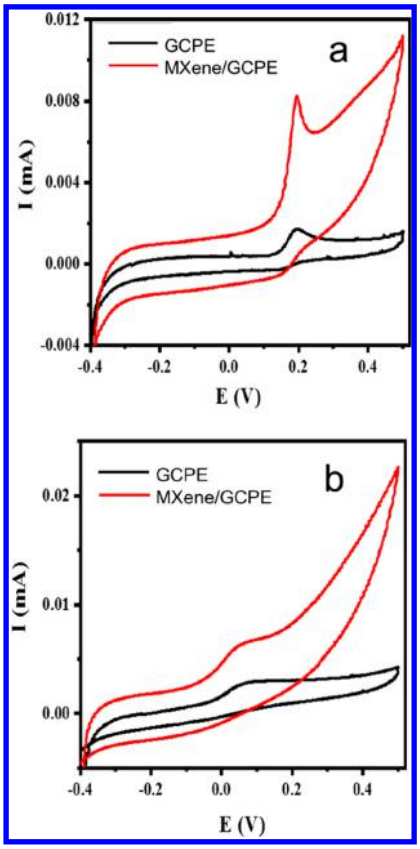

Figure 8. (a) CVs obtained for the oxidation of 10 μM AA in 0.2 M PBS of pH 7.4 at GCPE and MXene/GCPE with a scan rate of 50 mV s^{-1}. (b) CVs obtained for the oxidation of 10 μM 5-HT in 0.2 M PBS of pH 7.4 at GCPE (−) and MXene/GCPE (−) with a scan rate of 50 mV s^{-1}.

oxidation peak of 10.0 μM 5-HT in PBS of pH 7.4 is obtained at about 0.193 V. Because of a slow electron-transfer kinetics, the generated peak on GCPE appears broad.[42] On the other hand, the oxidation peak of 5-HT on the modified electrode also appears at the same potential (0.197 V). However, the peak becomes sharp, and the peak current enhances considerably. Figure 5b shows the CVs of oxidation of 10.0 μM AA at the bare and modified electrodes in PBS (7.4 pH) solution with a scan rate of 50 mV s^{-1}. AA exhibits an oxidation peak at 0.094 V with an irreversible electrochemical behavior at the bare GCPE. As compared to the bare GCPE, the peak current of AA was higher on the fabricated electrode. Moreover, the oxidation potential of AA was also shifted to a slightly negative side on GCPE. From all these discussions, it can be concluded that the modified electrode accelerates the electron-transfer process of both AA and 5-HT oxidation.[43]

DOI: 10.1021/acsami.8b11741
ACS Appl. Mater. Interfaces 2018, 10, 43343−43351

The scan rate effects on the electrochemical oxidation of individual AA and 5-HT in PBS on bare and MXene-modified electrodes were plotted and studied (Figures S6(a–c)–S9(a–c)). The studies reveal that the peak current due to the oxidation of AA and 5-HT are proportional to scan rates. Further analysis of the plot of the square root of the scan rate with peak current suggests that the electrode reaction was controlled by a diffusion process. Dependence of pH toward the oxidation of AA and 5-HT were also analyzed with the modified electrode (Figures S10a,b and S11a,b). In both cases, a maximum current response was obtained for PBS of 7.4 pH.

CVs of the ternary mixture consisting of 10 μM AA, 1 μM AD, and 10 μM 5-HT at the GCPE and MXene-modified electrode were recorded in the PBS of pH 7.4 (Figure 9a).

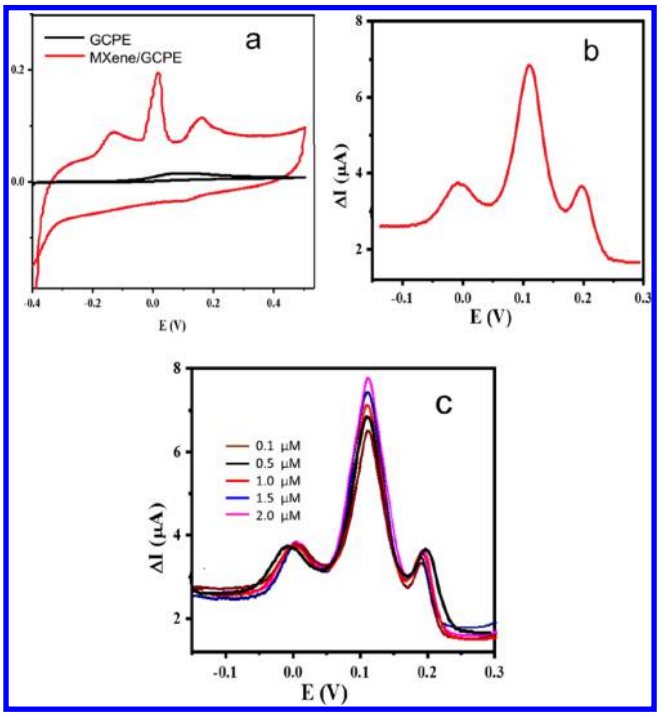

Figure 9. (a) CVs obtained at GCPE (a) and MXene/GCPE (b) in 0.2 M PBS of pH 7.4 containing a mixture of 0.1 μM AD and 10 μM AA and 10 μM 5-HT at a scan rate 50 mV s^{-1}. (b) DPV of MXene/GCPE in 0.2 M PBS of pH 7.4 containing 0.1 μM AD and 10 μM AA and 10 μM 5-HT at a scan rate 50 mV s^{-1}. (c) DPVs of different concentration of AD (0.1–2 μM) in presence of constant AA (10 μM) and 5-HT (10 μM) at scan rate of 20 mV s^{-1}.

Because of high electrocatalytic properties and large electroactive surface area of MXene-modified electrode, three distinct anodic peaks at −0.12, 0.02, and 0.18 V corresponding to AA, AD, and 5-HT were observed. The peak-to-peak separations were 0.1, 0.16, and 0.19 V for AA/AD, AD/5-HT, and AA/5-HT, respectively. At the GCPE a broad oxidation peak was observed at 0.1 V, and the bare electrode could separate the individual peaks from AA, AD, and 5-HT.[44] These results confirmed that MXene/GCPE exhibits selective electrocatalytic behavior for simultaneous electro analysis of AA, AD, and 5-HT.

Differential pulse voltammetry was also performed to confirm the ability for simultaneous detection of the modified electrode for 10 μM AA, 1.0 μM AD, and 10 μM 5-HT. The DPV curves (Figure 9b) show that the MXene-modified electrode can clearly distinguish these three substances separately. All peaks are separated by at least 0.08 V. The voltammetric peaks of AA, AD, and 5-HT appear at 0.01, 0.11, and 0.19 V, respectively. The anodic peak separations for AA/AD, AD/5-HT, and AA/5-HT are 0.1, 0.08, and 0.18 V, respectively. These separations between the voltammetric peaks are clear enough to distinguish these three substances. DPVs of different concentrations of AD (0.1–2 μM) in the presence of a constant amount of AA (10 μM) and 5-HT (10 μM) were measured and plotted at a scan rate of 20 mV s^{-1} (Figure 9c). The increase in the concentration of AD from 0.1 to 2 μM leads to the increase in peak current corresponding to AD. The peak currents and peak potentials of AA and 5-HT remain unaltered during the increase in the concentration of AD.

Interference studies of AA were carried out by changing the concentration from 2 to 200 mM with 1 μM AD and 10 mM 5-HT in PBS (pH 7.4). Similarly, the interference of 5-HT in the range of 1–200 mM in 10 mM AA and 1 μM AD were also analyzed. In both the cases, the current corresponding to AA and 5-HT increased proportionally to a correlation coefficient of 0.999 and 0.998, respectively. Therefore, there is no hindrance in the determination of the 5-HT or AA in a coexisting state. These results strongly suggest that MXene/GCPE electrode is capable of determining AD, AA, and 5-HT from their ternary mixture separately.

Ten repetitive measurements for the sensing of AD and 5-HT were carried out using the fabricated MXene/GCPE to check the reproducibility, and it was observed that the AD and 5-HT oxidation peak currents remain unaltered. In both the cases, 99% of original current response was retained. Further, the MXene/GCPE was monitored for long-term stability by measuring the CV in 10 days' intervals, for 30 days. The sensor was washed, dried, and stored at room temperature after every experiment. After 30 days, it was noted that the fabricated electrode retained 98% of its initial current response to AD and 5-HT. Comparison of the fabricated MXene/GCPE with reported modified electrodes and methods is presented in

Table 1. Comparison of MXene/GCPE with Reported Modified Electrodes and Methods towards the Detection of AD

electrode	detection limit (μM)	linear range	method	references
zeolite-modified carbon paste electrode doped with iron(III) (Fe^{3+}Y/ZMCPE)	0.44	0.9–216 μM	DPV	46
mesoporous SiO_2-modified carbon paste electrode	0.6	0.1–60 μM	CV	47
ferrocene-modified CNT paste electrode	0.2	0.5–200 μM	DPV	48
multiwalled CNT-modified carbon paste electrode	0.029	0.03–500 μM	DPV	49
NiO/CNTs nanocomposite-modified carbon paste electrode (CPE/NiO/CNTs)	0.01	0.08–900 μM	SWV	50
niacin film-coated carbon paste electrode (niacin/CPE)	0.011	20.6–174.4 μM	CV	51
hydroquinone derivative and graphene oxide nanosheet-modified carbon paste electrode	0.65	1.5–600 μM	DPV	52
MXene/GCPE	*0.009*	*0.02–10 μm, 10–100 μm*	*CA*	*this work*

DOI: 10.1021/acsami.8b11741
ACS Appl. Mater. Interfaces 2018, 10, 43343–43351

Table 1. To the best of our knowledge, among the carbon-based electrodes, detection limit of 9.5 nM achieved by using the MXene/GCPEs is the best toward the AD detection.[45]

The developed MXene/GCPE sensor was evaluated for its applicability in the determination of AD in AD injection samples along with its recovery measurements. AD samples with different concentrations were prepared by dilution of AD tartrate ampoule contents (5 mL of 1 mg/mL AD tartrate injection from Hindustan Pharmaceuticals India Ltd) with PBS (pH 7.4). Then, each sample was tested in an electrochemical cell for the determination of its AD content followed by analysis using the fabricated sensor (Table 2). The calculation

Table 2. Detection of AD from AD Bitartrate Injection Using MXene/GCPE

samples	added (μg mL^{-1})	found (μg mL^{-1})	RSD (%)	recovery rate (%)
1	2	2.06 ± 0.05	0.07	101.5
2	3	2.98 ± 0.03	0.04	99.3
3	4	4.17 ± 0.03	0.34	104.2

of real sample concentration with S/N of 3 was done by standard addition method. The results indicate that the employed method is very efficient for the determination of AD.

CONCLUSIONS

2D Ti_2CT_xMXene was prepared by the selective etching of Ti_2AlC MAX phase for the fabrication of MXene/GCPE. The electrochemical characterization of the MXene/GCPE electrode was carried out with the ferri/ferrocyanide system in KCl. Studies revealed that the electron-transfer rate was improved in the presence of MXenes. The MXene/GCPE sensor exhibited a high sensitivity towards AD with a low detection limit of 9.5 nM. Simultaneous and individual analysis of AD, serotonin and AA was successfully achieved with the sensor with a considerable peak-to-peak separation. Furthermore, the fabricated MXene/GCPE electrode was successfully employed for the analysis of adrenalin in samples, suggesting the potential of the electrode sensor for practical applications.

ASSOCIATED CONTENT

Supporting Information

The Supporting Information is available free of charge on the ACS Publications website at DOI: 10.1021/acsami.8b11741.

Plot of current versus concentration of MXene (from 5 to 30 mg) in 1 mM $K_3Fe(CN)_6$ and 0.1 M KCl with a scan rate 50 mV s^{-1}, CVs of MXene/GCPE and bare in 1 mM $K_3Fe(CN)_6$ and 0.1 M KCl, CVs of 1.0 μM NE in 0.2 M PBS of pH 7.4 at MXene/GCPE and bare GCPE with various scan rates, CVs of 1.0 μM AA in 0.2 M PBS of pH 7.4 at MXene/GCPE and bare GCPE with various scan rates, CVs of 1.0 μM 5-HT in 0.2 M PBS of pH 7.4 at MXene/GCPE and bare GCPE with various scan rates, CVs obtained for 1.0 μM 5-HT with the MXene/GCPE in 0.2 M PBS with pH values, CVs obtained for 1.0 μM AA with the MXene/GCPE in 0.2 M PBS with pH values (PDF)

AUTHOR INFORMATION

Corresponding Authors

*E-mail: sharathshankar82@gmail.com (S.S.S.).

*E-mail: rakhiraghavanbaby@niist.res.in (R.B.R.).

ORCID

R. B. Rakhi: 0000-0002-0207-8595

Notes

The authors declare no competing financial interest.

ACKNOWLEDGMENTS

S.S.S. acknowledges the support from KSCSTE, Govt. of Kerala. R.B.R. acknowledges the support of Ramanujan Fellowship, Department of Science and Technology (DST), Govt. of India and CSIR-NIIST Thiruvananthapuram, India.

REFERENCES

(1) Lei, J.-C.; Zhang, X.; Zhou, Z. Recent Advances in MXene: Preparation, Properties, and Applications. *Front. Phys.* **2015**, *10*, 276–286.

(2) Naguib, M.; Mochalin, V. N.; Barsoum, M. W.; Gogotsi, Y. 25th Anniversary Article: MXenes: A New Family of Two-Dimensional Materials. *Adv. Mater.* **2014**, *26*, 992–1005.

(3) Naguib, M.; Mashtalir, O.; Carle, J.; Presser, V.; Lu, J.; Hultman, L.; Gogotsi, Y.; Barsoum, M. W. Two-Dimensional Transition Metal Carbides. *ACS Nano* **2012**, *6*, 1322–1331.

(4) Ling, Z.; Ren, C. E.; Zhao, M.-Q.; Yang, J.; Giammarco, J. M.; Qiu, J.; Barsoum, M. W.; Gogotsi, Y. Flexible and Conductive MXene Films and Nanocomposites with High Capacitance. *Proc. Natl. Acad. Sci. U.S.A.* **2014**, *111*, 16676.

(5) Lukatskaya, M. R.; Mashtalir, O.; Ren, C. E.; Dall'Agnese, Y.; Rozier, P.; Taberna, P. L.; Naguib, M.; Simon, P.; Barsoum, M. W.; Gogotsi, Y. Cation Intercalation and High Volumetric Capacitance of Two-Dimensional Titanium Carbide. *Science* **2013**, *341*, 1502.

(6) Naguib, M.; Come, J.; Dyatkin, B.; Presser, V.; Taberna, P.-L.; Simon, P.; Barsoum, M. W.; Gogotsi, Y. MXene: a Promising Transition Metal Carbide Anode for Lithium-Ion Batteries. *Electrochem. Commun.* **2012**, *16*, 61–64.

(7) Liu, H.; Duan, C.; Yang, C.; Shen, W.; Wang, F.; Zhu, Z. A Novel Nitrite Biosensor Based on the Direct Electrochemistry of Hemoglobin Immobilized on MXene-Ti3C2. *Sens. Actuators, B* **2015**, *218*, 60–66.

(8) Wang, F.; Yang, C.; Duan, C.; Xiao, D.; Tang, Y.; Zhu, J. An Organ-Like Titanium Carbide Material (MXene) with Multilayer Structure Encapsulating Hemoglobin for a Mediator-Free Biosensor. *J. Electrochem. Soc.* **2015**, *162*, B16–B21.

(9) Wang, F.; Yang, C.; Duan, M.; Tang, Y.; Zhu, J. TiO 2 nanoparticle modified organ-like Ti 3 C 2 MXene nanocomposite encapsulating hemoglobin for a mediator-free biosensor with excellent performances. *Biosens. Bioelectron.* **2015**, *74*, 1022–1028.

(10) Rakhi, R. B.; Nayak, P.; Xia, C.; Alshareef, H. N. Novel Amperometric Glucose Biosensor Based on MXene Nanocomposite. *Sci. Rep.* **2016**, *6*, 36422. https://www.nature.com/articles/srep36422#supplementary-information

(11) Ren, W.; Luo, H.; Li, N. Electrochemical Behavior of Epinephrine at a Glassy Carbon Electrode Modified by Electrodeposited Films of Caffeic Acid. *Sensors* **2006**, *6*, 80.

(12) Izaoumen, N.; Bouchta, D.; Zejli, H.; El Kaoutit, M.; Temsamani, K. R. The Electrochemical Behavior of Neurotransmitters at a Poly (Pyrrole- β-Cyclodextrin) Modified Glassy Carbon Electrode. *Anal. Lett.* **2005**, *38*, 1869–1885.

(13) Al-Ameri, S. A. H. Spectrophotometric Determination of Adrenaline in Pharmaceutical Preparations. *Arabian J. Chem.* **2016**, *9*, S1000–S1004.

(14) Verberne, A. J. M.; Korim, W. S.; Sabetghadam, A.; Llewellyn-Smith, I. J. Adrenaline: Insights into its Metabolic Roles in Hypoglycaemia and Diabetes. *Br. J. Pharmacol.* **2016**, *173*, 1425–1437.

(15) Carter, J. R.; Goldstein, D. S. Sympathoneural and Adrenomedullary Responses to Mental Stress. *Compr. Physiol.* **2015**, *5*, 119–146.

DOI: 10.1021/acsami.8b11741
ACS Appl. Mater. Interfaces 2018, 10, 43343–43351

(16) Rosochacki, S. J.; Piekarzewska, A. B.; Połoszynowicz, J.; Sakowski, T. The Influence of Restraint Immobilization Stress on the Concentration qf Bioamines and Cortisol in Plasma of Pietrain and Duroc Pigs. *J. Vet. Med., A* **2000**, *47*, 231−242.
(17) Queiroz, D.; Dadamos, T.; Machado, S.; Martines, M. Electrochemical Determination of Norepinephrine by Means of Modified Glassy Carbon Electrodes with Carbon Nanotubes and Magnetic Nanoparticles of Cobalt Ferrite. *Sensors* **2018**, *18*, 1223.
(18) Tavakkoli, N.; Soltani, N.; Shahdost-fard, F.; Ramezani, M.; Salavati, H.; Jalali, M. R. Simultaneous Voltammetric Sensing of Acetaminophen, Epinephrine and Melatonin Using a Carbon Paste Electrode Modified with Zinc Ferrite Nanoparticles. *Microchim. Acta* **2018**, *185*, 479.
(19) Zaidi, S. A. Utilization of an Environmentally-Friendly Monomer for an Efficient and Sustainable Adrenaline Imprinted Electrochemical Sensor Using Graphene. *Electrochim. Acta* **2018**, *274*, 370−377.
(20) Ni, F.; Wang, Y.; Zhang, D.; Gao, F.; Li, M. Electrochemical Oxidation of Epinephrine and Uric Acid at a Layered Double Hydroxide Film Modified Glassy Carbon Electrode and Its Application. *Electroanalysis* **2010**, *22*, 1130−1135.
(21) Aslanoglu, M.; Kutluay, A.; Karabulut, S.; Abbasoglu, S. Voltammetric Determination of Adrenaline Using a Poly(1-Methylpyrrole) Modified Glassy Carbon Electrode. *J. Chin. Chem. Soc.* **2008**, *55*, 794−800.
(22) Liu, H.; Zhao, G.; Wen, L.; Ye, B. Simultaneous Voltammetric Determination of Epinephrine and Serotonin at a p-tetra-butyl calix [6] arene-L-Histidine Chemically Modified Electrode. *J. Anal. Chem.* **2006**, *61*, 1104−1107.
(23) Mphuthi, N. G.; Adekunle, A. S.; Ebenso, E. E. Electrocatalytic Oxidation of Epinephrine and Norepinephrine at Metal Oxide Doped Phthalocyanine/MWCNT Composite Sensor. *Sci. Rep.* **2016**, *6*, 26938. https://www.nature.com/articles/srep26938#supplementary-information
(24) Venton, B. J.; Wightman, R. M. Psychoanalytical Electrochemistry: Dopamine and Behavior. *Anal. Chem.* **2003**, *75*, 414A−421A.
(25) Perry, M.; Li, Q.; Kennedy, R. T. Review of Recent Advances in Analytical Techniques for the Determination of Neurotransmitters. *Anal. Chim. Acta* **2009**, *653*, 1−22.
(26) Rakhi, R. B.; Ahmed, B.; Hedhili, M. N.; Anjum, D. H.; Alshareef, H. N. Effect of Postetch Annealing Gas Composition on the Structural and Electrochemical Properties of Ti2CTx MXene Electrodes for Supercapacitor Applications. *Chem. Mater.* **2015**, *27*, 5314−5323.
(27) Ndlovu, T.; Arotiba, O. A.; Sampath, S.; Krause, R. W.; Mamba, B. B. Reactivities of Modified and Unmodified Exfoliated Graphite Electrodes in Selected Redox Systems. *Int. J. Electrochem. Sci.* **2012**, *7*, 9441−9453.
(28) Naguib, M.; Kurtoglu, M.; Presser, V.; Lu, J.; Niu, J.; Heon, M.; Hultman, L.; Gogotsi, Y.; Barsoum, M. W. Two-Dimensional Nanocrystals Produced by Exfoliation of Ti3AlC2. *Adv. Mater.* **2011**, *23*, 4248−4253.
(29) Viculis, L. M.; Mack, J. J.; Mayer, O. M.; Hahn, H. T.; Kaner, R. B. Intercalation and Exfoliation Routes to Graphite Nanoplatelets. *J. Mater. Chem.* **2005**, *15*, 974−978.
(30) Mitchell, D. R. G. Circular Hough transform diffraction analysis: A software tool for automated measurement of selected area electron diffraction patterns within Digital Micrograph. *Ultramicroscopy* **2008**, *108*, 367−374.
(31) Walter, E. C.; Beetz, T.; Sfeir, M. Y.; Brus, L. E.; Steigerwald, M. L. Crystalline Graphite from an Organometallic Solution-Phase Reaction. *J. Am. Chem. Soc.* **2006**, *128*, 15590−15591.
(32) Jia, F.; Yu, C.; Ai, Z.; Zhang, L. Fabrication of Nanoporous Gold Film Electrodes with Ultrahigh Surface Area and Electrochemical Activity. *Chem. Mater.* **2007**, *19*, 3648−3653.
(33) Hu, H.; Feng, M.; Zhan, H. A Glucose Biosensor Based on Partially Unzipped Carbon Nanotubes. *Talanta* **2015**, *141*, 66−72.
(34) Dutta, D.; Chandra, S.; Swain, A. K.; Bahadur, D. SnO2 Quantum Dots-Reduced Graphene Oxide Composite for Enzyme-Free Ultrasensitive Electrochemical Detection of Urea. *Anal. Chem.* **2014**, *86*, 5914−5921.
(35) Ma, H.; He, J.; Xiong, D.-B.; Wu, J.; Li, Q.; Dravid, V.; Zhao, Y. Nickel Cobalt Hydroxide @Reduced Graphene Oxide Hybrid Nanolayers for High Performance Asymmetric Supercapacitors with Remarkable Cycling Stability. *ACS Appl. Mater. Interfaces* **2016**, *8*, 1992−2000.
(36) Nambiar, S. R.; Aneesh, P. K.; Rao, T. P. Ultrasensitive Voltammetric Determination of Catechol at a Gold Atomic Cluster/poly(3,4-ethylenedioxythiophene) Nanocomposite electrode. *Analyst* **2013**, *138*, 5031−5038.
(37) Shereema, R. M.; Sankar, V.; Raghu, K. G.; Rao, T. P.; Shankar, S. S. One Step Green Synthesis of Carbon Quantum Dots and its Application Towards the Bioelectroanalytical and Biolabeling Studies. *Electrochim. Acta* **2015**, *182*, 588−595.
(38) Watanabe, T.; Ivandini, T. A.; Makide, Y.; Fujishima, A.; Einaga, Y. Selective Detection Method Derived from a Controlled Diffusion Process at Metal-Modified Diamond Electrodes. *Anal. Chem.* **2006**, *78*, 7857−7860.
(39) Liu, L.; Zhou, Y.; Liu, S.; Xu, M. The Applications of Metal−Organic Frameworks in Electrochemical Sensors. *ChemElectroChem* **2018**, *5*, 6−19.
(40) Zhou, W.-H.; Wang, H.-H.; Li, W.-T.; Guo, X.-C.; Kou, D.-X.; Zhou, Z.-J.; Meng, Y.-N.; Tian, Q.-W.; Wu, S.-X. Gold Nanoparticles Sensitized ZnO Nanorods Arrays for Dopamine Electrochemical Sensing. *J. Electrochem. Soc.* **2018**, *165*, G3001−G3007.
(41) Sochr, J.; Švorc, L′.; Rievaj, M.; Bustin, D. Electrochemical Determination of Adrenaline in Human Urine Using a Boron-Doped Diamond Film Electrode. *Diamond Relat. Mater.* **2014**, *43*, 5−11.
(42) Wang, L.; Huang, P.; Bai, J.; Wang, H.; Wu, X.; Zhao, Y. Voltammetric Sensing of Uric Acid and Ascorbic Acid with Poly (p-toluene sulfonic acid) Modified Electrode. *Int. J. Electrochem. Sci.* **2006**, *1*, 334−342.
(43) Chen, S.-M.; Liu, J.-W.; Thangamuthu, T. Preparation, Characterization and Electrocatalytic Studies on Copper Complex Dye Film Modified Electrodes. *Electroanalysis* **2007**, *19*, 1429−1436.
(44) Xu, H.; Wang, L.; Luo, J.; Song, Y.; Liu, J.; Zhang, S.; Cai, X. Selective Recognition of 5-Hydroxytryptamine and Dopamine on a Multi-Walled Carbon Nanotube-Chitosan Hybrid Film-Modified Microelectrode Array. *Sensors* **2015**, *15*, 1008−1021.
(45) Vytřas, K.; Svancara, I.; Metelka, R. Carbon Paste Electrodes in Electroanalytical Chemistry. *J. Serb. Chem. Soc.* **2009**, *74*, 1021−1033.
(46) Babaei, A.; Mirzakhani, S.; Khalilzadeh, B. A Sensitive Simultaneous Determination of Epinephrine and Tyrosine using an Iron(III) Doped Zeolite-Modified Carbon Paste Electrode. *J. Braz. Chem. Soc.* **2009**, *20*, 1862−1869.
(47) Yi, H.; Li, Z.; Li, K. Application of Mesoporous SiO2-Modified Carbon Paste Electrode for Voltammetric Determination of Epinephrine. *Russ. J. Electrochem.* **2013**, *49*, 1073−1080.
(48) Akhgar, M. R.; Beitollahi, H.; Salari, M.; Karimi-Maleh, H.; Zamani, H. Fabrication of a Sensor for Simultaneous Determination of Norepinephrine, Acetaminophen and Tryptophan Using a Modified Carbon Nanotube Paste Electrode. *Anal. Methods* **2012**, *4*, 259−264.
(49) Thomas, T.; Mascarenhas, R. J.; Martis, P.; Mekhalif, Z.; Swamy, B. E. K. Multi-Walled Carbon Nanotube Modified Carbon Paste Electrode as an Electrochemical Sensor for the Determination of Epinephrine in the Presence of Ascorbic Acid and Uric Acid. *Mater. Sci. Eng., C* **2013**, *33*, 3294−3302.
(50) Gupta, V. K.; Mahmoody, H.; Karimi, F.; Agarwal, S.; Abbasghorbani, M. Electrochemical Determination of Adrenaline Using Voltammetric Sensor Employing NiO/CNTs Based Carbon Paste Electrode. *Int. J. Electrochem. Sci.* **2017**, *12*, 248−257.
(51) Teradale, A. B.; Lamani, S. D.; Ganesh, P. S.; Kumara Swamy, B. E.; Das, S. N. Niacin Film Coated Carbon Paste Electrode Sensor for the Determination of Epinephrine in Presence of Uric Acid: A Cyclic Voltammetric Study. *Anal. Chem. Lett.* **2017**, *7*, 748−764.

DOI: 10.1021/acsami.8b11741
ACS Appl. Mater. Interfaces 2018, 10, 43343−43351

(52) Tezerjani, M. D.; Benvidi, A.; Dehghani Firouzabadi, A.; Mazloum-Ardakani, M.; Akbari, A. Epinephrine electrochemical sensor based on a carbon paste electrode modified with hydroquinone derivative and graphene oxide nano-sheets: Simultaneous determination of epinephrine, acetaminophen and dopamine. *Measurement* **2017**, *101*, 183−189.

DOI: 10.1021/acsami.8b11741
ACS Appl. Mater. Interfaces 2018, 10, 43343−43351